Cell Reports

Article

Incoming HIV virion-derived Gag Spacer Peptide 2 (p1) is a target of effective CD8+ T cell antiviral responses

Graphical abstract

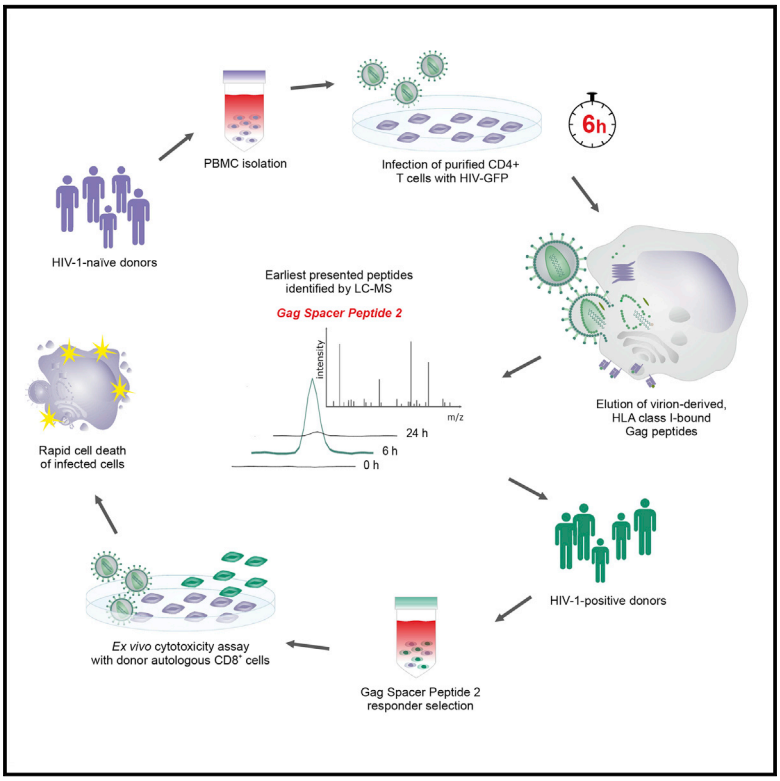

Highlights

- CD8+ T cell recognition of incoming HIV antigens leads to efficient virus control
- HLA-I-bound HIV peptides from incoming virions are identifiable by mass spectrometry
- Gag Spacer Peptide 2 elicits killing of CD4+ T cells early in the viral life cycle
- Early CD8+ T cell killing is not dependent on protective HLA class I alleles

Authors

Hongbing Yang, Anuska Llano, Samandhy Cedeño, ..., Nicola Ternette, Lucy Dorrell, Research in Viral Eradication of Reservoirs (RIVER) trial study group

Correspondence

hongbing.yang@ndm.ox.ac.uk (H.Y.), lucy.dorrell@ndm.ox.ac.uk (L.D.)

In brief

Unbiased approaches to deciphering immune control mechanisms in people with HIV may help in the search for a cure. Yang et al. use proteomics to identify viral peptides presented early in the viral life cycle and show that Gag Spacer Peptide 2 recognition triggers efficient CD8+ T cell killing.

Yang et al., 2021, Cell Reports *35*, 109103
May 11, 2021
https://doi.org/10.1016/j.celrep.2021.109103

CellPress

Cell Reports

CellPress
OPEN ACCESS

Article

Incoming HIV virion-derived Gag Spacer Peptide 2 (p1) is a target of effective CD8+ T cell antiviral responses

Hongbing Yang,[1,2,12,13,*] Anuska Llano,[3] Samandhy Cedeño,[3] Annette von Delft,[2,4] Angelica Corcuera,[1] Geraldine M. Gillespie,[1] Andrew Knox,[5] Darren B. Leneghan,[5] John Frater,[1,2,12] Wolfgang Stöhr,[6,12] Sarah Fidler,[7,12] Beatriz Mothe,[3,8,9] Johnson Mak,[10] Christian Brander,[3,8,11] Nicola Ternette,[1] Lucy Dorrell,[1,2,5,12,*] and Research in Viral Eradication of Reservoirs (RIVER) trial study group

[1]Nuffield Department of Medicine, University of Oxford, Oxford OX3 7FZ, UK
[2]National Institute for Health Research Oxford Biomedical Research Centre, University of Oxford, Oxford OX4 2PG, UK
[3]Irsicaixa AIDS Research Institute–HIVACAT, Hospital Universitari Germans Trias i Pujol, 08916 Badalona, Spain
[4]Centre for Medicines Discovery, University of Oxford, Oxford, UK
[5]Immunocore Ltd, Milton, Abingdon OX14 4RY, UK
[6]Medical Research Council Clinical Trials Unit, University College London, London WC1V 6LJ, UK
[7]Department of Infectious Disease, Imperial College London, National Institute for Health Research Imperial Biomedical Research Centre, London W2 1NY, UK
[8]Faculty of Medicine, Universitat de Vic-Central de Catalunya (UVic-UCC), 08500 Vic, Spain
[9]Fundacio Lluita contra la Sida, Infectious Disease Department, Hospital Universitari Germans Trias i Pujol, 08916 Badalona, Spain
[10]Institute for Glycomics, Griffith University Gold Coast, Southport QLD 4215, Australia
[11]Institució Catalana de Recerca I Estudis Avançats (ICREA), 08010 Barcelona, Spain
[12]Research In Viral Eradication of Reservoirs (RIVER) trial study group
[13]Lead contact
*Correspondence: hongbing.yang@ndm.ox.ac.uk (H.Y.), lucy.dorrell@ndm.ox.ac.uk (L.D.)
https://doi.org/10.1016/j.celrep.2021.109103

SUMMARY

Persistence of HIV through integration into host DNA in CD4+ T cells presents a major barrier to virus eradication. Viral integration may be curtailed when CD8+ T cells are triggered to kill infected CD4+ T cells through recognition of histocompatibility leukocyte antigen (HLA) class I-bound peptides derived from incoming virions. However, this has been reported only in individuals with "beneficial" HLA alleles that are associated with superior HIV control. Through interrogation of the pre-integration immunopeptidome, we obtain proof of early presentation of a virion-derived HLA-A*02:01-restricted epitope, FLGKIWPSH (FH9), located in Gag Spacer Peptide 2 (SP2). FH9-specific CD8+ T cell responses are detectable in individuals with primary HIV infection and eliminate HIV-infected CD4+ T cells prior to virus production *in vitro*. Our data show that non-beneficial HLA class I alleles can elicit an effective antiviral response through early presentation of HIV virion-derived epitopes and also demonstrate the importance of SP2 as an immune target.

INTRODUCTION

Antiretroviral therapy (ART) effectively suppresses HIV replication, yet treatment is not curative once infection is established in the host. Cellular reservoirs are established following integration of reverse transcribed HIV RNA into host DNA, enabling it to persist in a latent state that is insensitive to ART (Finzi et al., 1997; Chun et al., 1997). Interruption of therapy permits transcription of integrated viral DNA, leading to resumption of virion production. Thus, lifelong adherence to ART is necessary.

HIV preferentially infects and replicates in activated CD4+ T cells, while infection of resting CD4+ T cells is generally restricted or abortive (Doitsh et al., 2010; Zack et al., 2013). However, completion of reverse transcription and integration in CD4+ T cells that are transitioning to a resting memory state may be a critical event in the formation of latent reservoirs, which are mostly established at or close to the time of ART initiation (Shan et al., 2017; Abrahams et al., 2019). Reservoirs are dominated by integrated proviruses that are genetically defective and incapable of producing virions, yet they may be transcriptionally active and translationally competent; the resulting gene products of these defective proviruses may act as a decoy to the adaptive immune system (Bruner et al., 2016; Pollack et al., 2017). By contrast, replication-competent proviruses, which constitute a tiny fraction of all proviruses, are largely transcriptionally silent during ART. The CD4+ T cell clones that harbor these inducible proviruses (typically 1 per million resting CD4+ T cells) are thought to persist as a result of homeostatic or antigen-driven proliferation (Chomont et al., 2009; Bui et al., 2017; Reeves et al., 2018). These rare cells therefore present a major challenge for host immune control or viral eradication

because they are invisible to cytolytic T cells unless viral proteins are synthesized, processed, and presented via histocompatibility leukocyte antigen (HLA) molecules (Shan et al., 2012).

Current vaccination strategies focus primarily on eliciting broadly neutralizing antibodies that can prevent HIV from gaining a foothold. Although plausible, the potential for early cell-mediated immune responses to contain infection from the outset has proved difficult to establish. Rare individuals who maintain low or undetectable HIV viral loads in the absence of ART (HIV controllers [HICs]) show particularly effective antiviral $CD8^+$ T cells in the chronic phase of infection and also have smaller cellular HIV reservoirs, whether defined by assays that quantify total or integrated proviruses or solely intact proviral DNA (Betts et al., 2006; Deeks and Walker, 2007; Lambotte et al., 2005; Graf et al., 2011; Kwaa et al., 2020). However, few HIC subjects have been studied during primary HIV infection (Goulder and Deeks, 2018). Immune targeting of infected $CD4^+$ T cells during the "intracellular eclipse phase" of the viral life cycle and prior to viral integration may be an important mechanism underlying these individuals' ability to achieve sustained control of HIV, because it could limit the seeding of HIV reservoirs during primary infection (Nelson et al., 2001; Buckheit et al., 2013). Evidence to support this notion comes from observations that Gag- and Pol-specific $CD8^+$ T cell lines from simian immunodeficiency virus (SIV)-infected macaques and HICs recognized *in vitro*-infected $CD4^+$ cell lines and activated or resting primary $CD4^+$ T cells while in this non-productive eclipse phase (Sacha et al., 2007a, 2007b; Payne et al., 2010; Kløverpris et al., 2013; Buckheit et al., 2013; Monel et al., 2019). From this, it has been inferred that $CD8^+$ T cell killing of non-productively infected $CD4^+$ T cells is dependent on presentation of HIV peptides derived from incoming virions shortly after completion of cellular entry. However, direct evidence for this is limited. Furthermore, the aforementioned studies have reported this phenomenon only in the context of HLA class I alleles that are known to be enriched in HICs (HLA-B*57:01, B*58:01, B*27:05). Approximately 30% "elite" HICs (those with plasma viral loads typically <50 copies/mL) and 40%–50% viremic HICs (viral loads <2,000–10,000 copies/mL) do not have any known beneficial alleles, and the mechanisms of control in these individuals are not fully defined (Emu et al., 2008; Pereyra et al., 2008; Mothe et al., 2011).

Here, we identified individuals without beneficial HLA class I alleles who showed efficient killing of autologous $CD4^+$ T cells within 24 h of HIV superinfection. By interrogating the HLA class I-associated immunopeptidome for HIV epitopes presented specifically in the intracellular eclipse phase of the viral life cycle, we identified an HLA-A*02:01-restricted Gag Spacer Peptide 2 (SP2, also known as p1) epitope, FLGKIWPSH (FH9), that is preferentially presented in the eclipse phase. This peptide has not previously been described as a 9-mer epitope, and very little is known about the function of SP2, beyond its role as a spacer between the nucleocapsid and p6 domains of the Gag polyprotein. We show that FH9-specific $CD8^+$ T cells efficiently eliminate infected $CD4^+$ T cells *in vitro*, before they start to produce new virions. Furthermore, we show that processing of a virion-derived protein may generate different epitopes from those produced post-transcriptionally, because FH9-specific $CD8^+$ T cells that did not cross-react with the 10-mer epitope were detected *in vivo*. Together, these results advance our understanding of the importance of SP2 as a therapeutic or vaccine target and provide a possible mechanism through which apparently non-beneficial HLA alleles influence host immune control of HIV.

RESULTS

Kinetics of HIV Gag expression in primary $CD4^+$ T cells during the intracellular eclipse phase

We first established an *in vitro* infection model to show that activated bulk primary $CD4^+$ T cells harboring HIV in the pre-integration phase after infection could be identified by detection of intracellular Gag prior to new virion production. To accomplish this, we used a GFP-labeled Nef-competent HIV isolate, NLAD8 EGFP IRES_Nef (hereafter referred to as HIV-GFP). Gag^+ cells could be detected by intracellular staining as early as 2 h post-viral entry, whereas GFP expression was detected after only 18 h. Therefore, HIV-infected cells in the intracellular eclipse phase (pre-integration) were identified as Gag^+GFP^- (Figures 1A and 1B), while productively infected cells were identified as Gag^+GFP^+. To confirm that the capsid is rapidly degraded prior to viral integration, we assessed Gag p24 abundance by western blot over a 24-h period following infection of primary $CD4^+$ T cells from a panel of 13 HIV-naive donors. This assay showed that the p24 signal declined significantly during this time frame (Figures 1C and 1D). In contrast, p41 expression and p55 expression increased over a time course of 120 h post-infection, consistent with the synthesis of HIV polyproteins after integration and viral gene transcription (Figure 1E; Figure S1). Furthermore, GFP expression could be blocked by the addition of a reverse transcriptase inhibitor (zidovudine) or an integrase inhibitor (raltegravir) immediately after spinoculation with HIV, whereas intracellular Gag expression was blocked only by inhibition of viral entry with a fusion inhibitor, T20 (Figure 1F). Together, these data confirmed that the p24 signal up to 18 h post-spinoculation was derived from incoming virions (Figure 1F).

Eclipse phase killing by $CD8^+$ T cells is an efficient control mechanism, irrespective of HLA class I haplotype

To investigate whether intracellular eclipse phase killing could be elicited by viral peptide presentation in the context of any HLA class I allele, we selected eight subjects with chronic HIV infection (CHI) and diverse genetic backgrounds, only one of whom (OXF3) had an HLA class I allele (HLA-B*58:01) with a previously defined association with early antigen presentation (Table S1, OXF1–8). Because the antiviral activity of circulating HIV-specific $CD8^+$ T cells declines with suppression of viremia, these subjects were sampled prior to ART initiation (Hancock et al., 2017; Fidler et al., 2020). Purified $CD4^+$ T cells from these subjects were superinfected with HIV-GFP and cultured with autologous freshly isolated $CD8^+$ T cells in independent, parallel experiments, to enable sampling over 2–72 h. Eclipse phase killing was determined from the reduction in Gag^+GFP^- cells in $CD4^+/CD8^+$ T cell co-cultures when compared with $CD4^+$ T cells cultured alone. Two individuals showed detectable killing as early as 2 h post-infection, and a further four subjects showed a response by 6 h, ranging from 5% to 36%. Infected cell killing approached peak values by 24 h in five of eight subjects

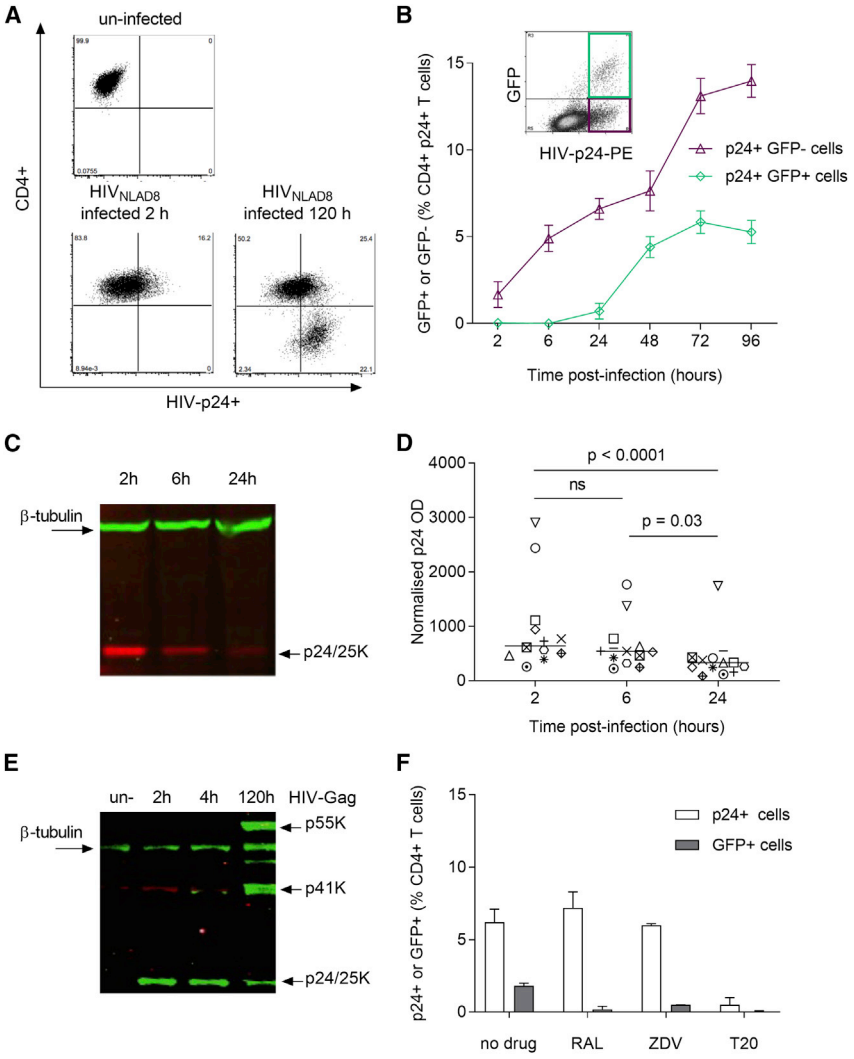

Figure 1. Detection of HIV-infected primary CD4$^+$ T cells in the intracellular eclipse phase

(A) Representative staining showing Gag p24 expression in mock-infected (top) and HIV-GFP-infected (NLAD8 EGFP IRES_Nef) CD4$^+$ T cells (bottom left and right).

(B) Frequency of Gag p24-positive GFP-negative and GFP-positive CD4$^+$ T cells after infection with HIV-GFP (MOI of 0.01) during 96-h culture. In the dot plot, p24$^+$ GFP$^-$ cells (bottom right quadrant) are in the intracellular eclipse phase.

(C and D) Representative western blot image showing relative abundance of Gag p24 (25k) (C) and normalized p24 optical density measured at 2, 6, and 24 h in HIV-GFP-infected CD4$^+$ T cells from 13 HIV-naive donors during 24-h culture with tenofovir disoproxil (1 μM) (D). Horizontal lines indicate median values. p values were obtained by Friedman's test with Dunn's post-test for multiple comparisons.

(E) Representative western blot image showing decrease in p24 expression from 2 to 120 h after HIV-GFP infection, with detection of Gag polyproteins p55k and p41, indicative of *de novo* protein synthesis at this time.

(F) Inhibition of viral integration and *de novo* protein synthesis, measured as % GFP$^+$ cells, in the presence of a reverse transcriptase inhibitor (zidovudine [ZDV]) or an integrase inhibitor (raltegravir [RAL]) when added immediately after infection. p24 expression was inhibited only by a fusion inhibitor, T20 (enfuvirtide), which blocks viral entry. The data shown were obtained 72 h post-infection.

(Figure 2A). Linear regression analysis showed that the percentage elimination value at 18 h post-infection accounted for 66% of the variation in the overall maximal killing observed ($p = 0.014$; Figure 2B). The 18-h time point was chosen for this analysis on the assumption that it represents the midpoint between the earliest possible effect of Nef on HLA class I expression (12 h post-infection) and the end of the eclipse phase (24 h; Figure 1B) (Sacha et al., 2007b; Althaus and De Boer, 2011). These data indicate that elimination of infected cells while in a non-productive state is an important determinant of HIV-specific CD8$^+$ T cell efficacy. Furthermore, although we did not map the viral epitopes targeted by CD8$^+$ T cells in these individuals, the data suggest that early killing may be elicited by a wider range of epitopes than has been previously suspected.

Identification of an HLA A*02:01-restricted 9-mer peptide, FLGKIWPSH (FH9), that is preferentially presented on HLA class I complexes during the intracellular eclipse phase

Next, we sought to confirm that HIV epitopes could be presented on the surface of CD4$^+$ T cells during the intracellular eclipse phase through direct elution and identification of HLA class I-associated peptides. We infected CD8-depleted peripheral blood mononuclear cells (PBMCs) from three HIV-naive donors with HIV-GFP virus at a multiplicity of infection (MOI) of 0.01 (cone 1: 120 million; cone 11: 90 million; cone 9: 105 million PBMCs) (Figure 3A). The frequencies of HIV-infected cells, as determined by intracellular p24 expression, in these samples were 29.8%, 32%, and 25%, respectively. Cells were lysed at 6 h and, for cone 11, also at 24 h post-infection (Figure 3A). Peptide-loaded HLA complexes were captured using the HLA class I-specific, conformation-dependent monoclonal antibody W6/32. HLA class I-associated peptides were isolated and analyzed by liquid chromatography-tandem mass spectrometry (LC-MS/MS), as described previously (Purcell et al., 2019). At 6 h, 1,811–3,799 unique peptides were identified in infected CD4$^+$ T cells from the three donors (Figure 3B). The majority were 8–12 amino acids long (94%, 95%, and 98% for the three donors, respectively), with 9-mers being the most abundant species (Figure 3C).

Overall, four unique HIV-derived peptides were identified (Table S2). The eluted HIV peptides at 6 h were derived from either Gag SP2 (3/3 donors) or Vpu (1 donor). In two donors, the same two Gag SP2 peptides were identified: a 9-mer FLGKIWPSH (FH9) and a 16-mer incorporating this sequence (FLGKIWPSHKGRPGNF) that represented the natural sequence

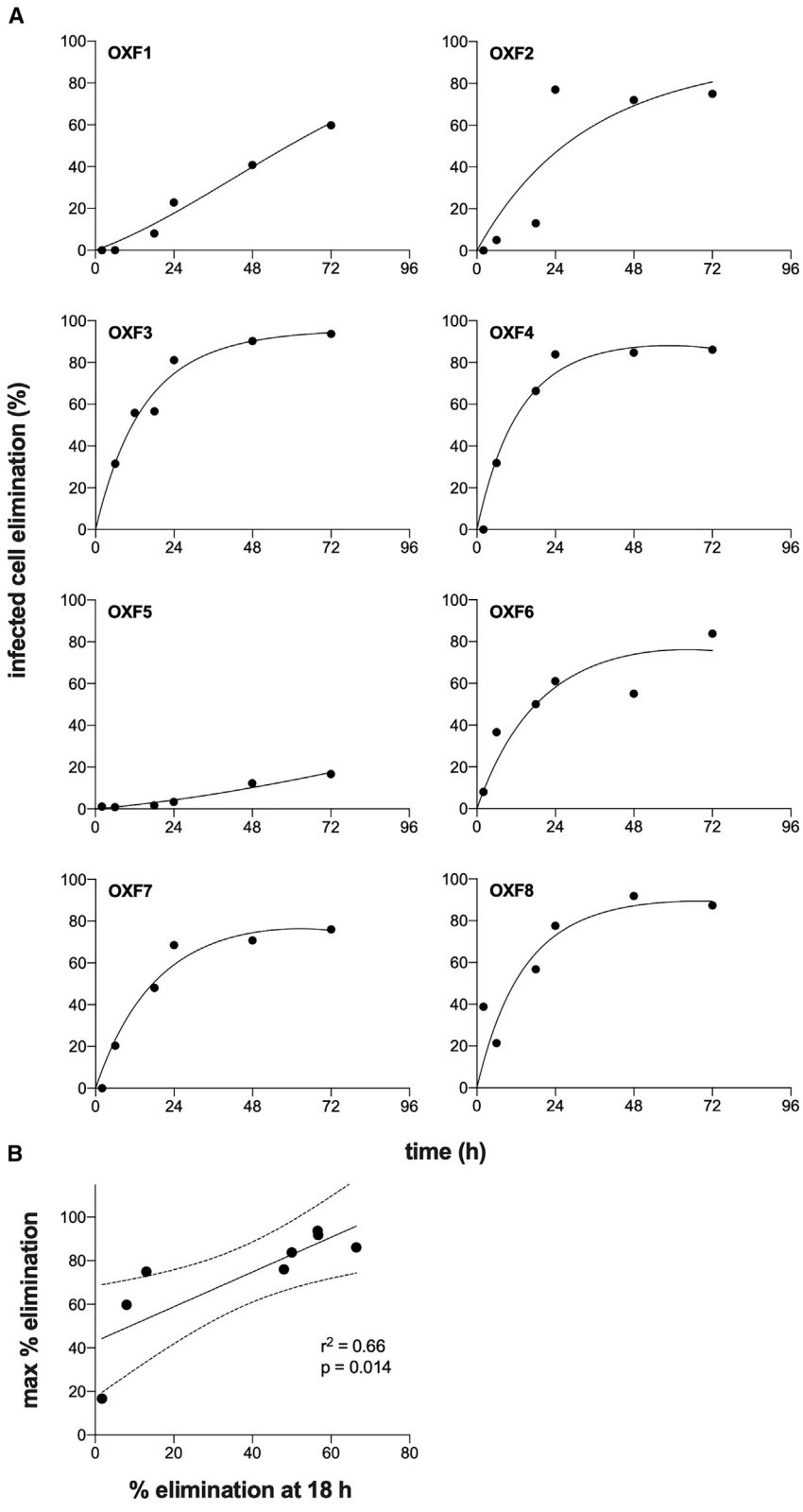

Figure 2. Kinetics of infected cell elimination by autologous CD8$^+$ T cells from ART-naive subjects with diverse HLA allotypes

(A) Elimination of HIV-GFP superinfected CD4$^+$ T cells by *ex vivo* autologous CD8$^+$ T cells (E:T = 1:1) from eight CHI ART-naive individuals. Independent co-cultures were sampled at 2, 6, 18, 24, 48, and 72 h, with additional sampling at 12 h in one individual; p24-positive cells were quantified by intracellular staining. Curve fitting was performed using the linear-quadratic model.

(B) Elimination values obtained in the 18-h culture were plotted against maximum % elimination (observed at 72 h in all subjects except OXF8, in which it occurred at 48 h). Best-fit values and 95% confidence bands are indicated by solid and dotted lines, respectively. OXF3: HLA-B*58:01 positive.

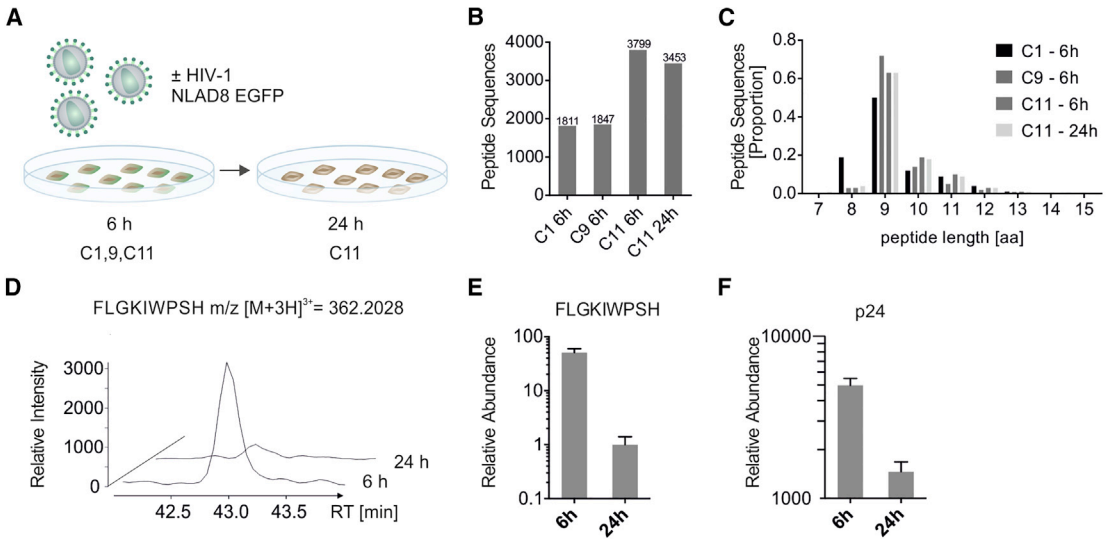

Figure 3. Identification of HIV peptides that are presented 6 h post-infection

(A) Schematic of the experimental layout.

(B) Number of identified peptide sequences in each sample.

(C) Length distribution of identified peptide sequences.

(D) FH9 peptide extracted ion chromatogram at 6 and 24 h (triply charged precursor, $m/z([M+3H]^{3+})$ = 362.2028). Curves show the relative intensities of the specific mass signal for the FH9 peptide eluting from the column over time (retention time [RT]).

(E) Relative abundance of the FH9 peptide in cone 11.

(F) Average intensity of tryptic peptides specific to p24 protein obtained in a tryptic digest of whole-cell lysate in cone 11.

of SP2. The latter peptide likely co-precipitated in these immunopeptidomic experiments because of membrane anchoring in infected cells, as previously reported (Partridge et al., 2018). We also identified an 8-mer variant, FLGKIWPS (FS8), in two donors and a Vpu-derived peptide, VALVVAIIIAIV, in one donor. Only one HIV peptide, the full-length SP2 sequence was identified in the 24-h-infected sample. The FS8 peptide has been reported previously as an HLA-A*02:01-restricted epitope (https://www.hiv.lanl.gov/content/immunology/), as have two 10-mer variants, FLGKIWPSHK (FK10, with a histidine at position 9) and FLGKIWPSYK (FK10, with a tyrosine at position 9). The majority (~95%) of clade B and C isolates carry the H9 variant (https://www.hiv.lanl.gov/content/index/). However, neither the FH9 nor the FY9 variants have been described before, although FY9 is reported to be immunogenic (Yu et al., 2002; Ternette et al., 2016). The abundance of FH9 at 6 h was >50-fold greater than at 24 h, with the 24-h signal being hardly detectable above background (Figures 3D and 3E). We also performed a tryptic digestion of the cell lysate-obtained proteins and determined the relative abundance of p24 protein by LC-MS/MS. In these experiments, p24 declined in cell lysates between 6 and 24 h, reflecting the intracellular delay in new Gag protein synthesis, as demonstrated in Figures 1C and 1D, and mirroring the decline in immunoprecipitated p24 HLA-bound peptides (Figures 3E and 3F).

Stable isotope labeling of amino acids in cell culture confirms incoming virions as the source of Gag SP2-derived peptide

To further confirm that the FLGKIWPSH peptide originated from incoming viral protein material rather than from newly synthesized viral protein, we performed stable isotope labeling by amino acids in cell culture (SILAC) of T0 cells (a T/B cell hybridoma, 90 million cells) with heavy lysine (K4) and heavy arginine (R10). We infected with the same unlabeled HIV-GFP isolate for 6 and 24 h or mock infected (0 h) (Figure 4A). LC-MS acquisition and analysis of a tryptic digestion of these samples confirmed 95% labeling efficiency in the samples. We then analyzed the immunopeptidome (Gag-positive T0 cell frequencies were 22.5% and 27.5%, respectively) and identified 5,883, 6,649, and 6,513 peptides in mock-infected cells (0-, 6- and 24-h-infected cells, respectively) (Figure 4B). The peptide length distribution was similar to that observed in primary cells at both the 6- and 24-h time points (Figure 4C). The peptide ion signal indicated the presence of unlabeled FH9 peptide at 6 h, which strongly supported its origin from incoming virions (Figure 4D). The HLA class I-presented FH9 peptide was again more abundant at 6 h than at 24 h (Figure 4E), matching the trajectory of the total p24 signal in a tryptic digestion of total extracted protein (Figure 4F). None of the six tryptic peptides matching to p24 were labeled, providing further evidence that p24 protein was sourced from incoming virions.

The Gag SP2 FH9 peptide binds to HLA-A*02:01

The previously described FK10 epitopes are known to bind to HLA-A*02, irrespective of variation at position 9 (Yu et al., 2002; Pereyra et al., 2014; Llano et al., 2019). Because the three HIV-negative donors in whom incoming virion-derived HIV peptides were identified were all HLA-A*02:01 positive, we predicted that this allele would also be the restriction element for FH9. However, although the leucine residue present in FH9 at position

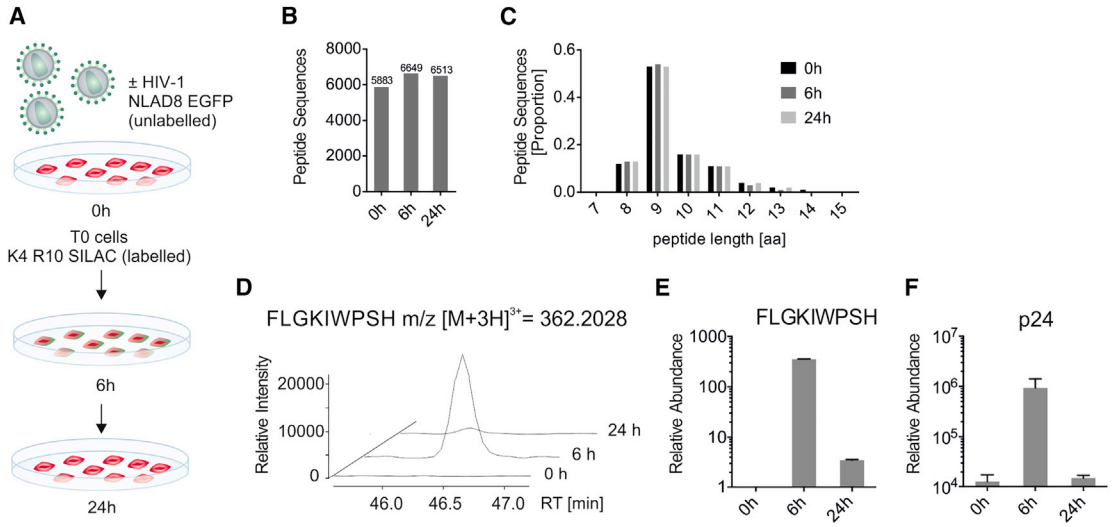

Figure 4. FH9 peptide does not originate from newly synthesized Gag proteins

(A) Schematic of the experimental layout using K4 and R10 isotope labeling.

(B) Number of distinct peptide sequences identified in each sample.

(C) Length distribution of identified peptide sequences.

(D) FH9 peptide extracted ion chromatogram at 6 and 24 h (unlabeled form, triply charged precursor, $m/z([M+3H]^{3+}) = 362.2028$). Curves show relative intensities of the specific mass signal for the FH9 peptide eluting from the column over time (RT).

(E) Relative abundance of the FH9 peptide in cone 11.

(F) Average intensity of tryptic peptides specific to p24 protein obtained in a tryptic digest of whole-cell lysate in indicated samples.

2 is predictive for binding to HLA-A*02:01, histidine (position 9) is an infrequent C-terminal anchor. To confirm binding of FH9 peptide to HLA-A*02:01, we refolded purified HLA-A*02:01 heavy chain and β_2-microglobulin with FH9 and assessed the stability of FH9 in HLA-A*02:01 by detection of ILT2 activity using surface plasmon resonance (Garboczi et al., 1992). The peptide binding affinities for FK10 and FS8 were also determined at the same time. The binding half-lives were 3.46, 7.98, and 16.92 h for FK10, FH9, and FS8, respectively (Figure 5A), demonstrating that FH9 binds strongly to HLA-A*02:01. We further confirmed FH9 binding by exogenous loading of HLA-A*02:01-expressing transporter associated with antigen processing (TAP)-deficient T2 cells, followed by detection of cell surface HLA-peptide complexes using a fluorophore-labeled HLA-A2 antibody. This assay indicated a fluorescence index (FI; net median fluorescence ratio of sample peptide to no peptide) of 3.07 for FH9, which compared favorably with the positive control peptide HIV Gag SL9 (SLFNTVATL; FI: 3.18) that is known to bind to HLA A*02:01 (Figure 5B), underscoring the efficient presentation of FH9 by HLA-A*02:01.

FH9-specific CD8$^+$ T cells are primed *in vivo* in chronic and primary HIV infection

T cell responses to FK10 have been frequently reported in individuals with CHI infection and have also been observed in acute infection (Yu et al., 2002; Streeck et al., 2009; Trautmann et al., 2012; Pereyra et al., 2014). We therefore tested PBMCs from 32 HLA-A*02:01-positive individuals, for recognition of the FH9 epitope, together with FK10, in interferon (IFN)-γ enzyme-linked immunoabsorbent spot (ELISpot) assays. The tested HIV-positive individuals were all virologically suppressed on ART (HIV RNA < 50 copies/mL, with the exception of OXF21, who had low-level viremia at the time of sampling) and were classified according to the timing of ART initiation: "PHI" subjects were those who had initiated ART at the time of or just prior to a confirmed diagnosis of primary HIV infection (criteria described in Fidler et al., 2020) and had been treated for at least 40 weeks at the time of sampling (n = 21); "CHI-ART" subjects had initiated ART in CHI (>6 months after acquisition) in accordance with contemporary treatment guidelines and had been treated for a median of 7 years (n = 11) (Tables S1, OXF9–21, and S3). The frequency of FH9 responders was 9/21 PHI (43%) and 3/11 CHI-ART (27%) (Figures 6A and 6B, respectively).

Because the majority of FH9 responders also recognized FK10, we wished to determine whether the detection of FH9-reactive T cells in either primary HIV infection or CHI could be explained by cross-reactivity of T cells primed by FK10, which from our analyses and published data is generated only post-transcriptionally (https://www.hiv.lanl.gov/content/immunology/). Because the frequency of circulating FK10-specific T cells was generally <0.05% in these ART-treated subjects (Figures 6A and 6B), we selected known responders to FK10 from a separate cohort of HLA-A*02:01-positive CHI subjects, the majority of whom were viremic at the time of sampling. This group comprised two non-controllers ("NCs") and five HICs (Table S1, BCN01–07). We then used phycoerythrin (PE)-labeled HLA-A*02:01-FH9 or -FK10 tetramers to stain *ex vivo* CD8$^+$ T cells from five of these responders (BCN01–05, selected according to sample availability; Figure 6C). Tetramer staining yielded frequencies ranging from 0.19% to 1.81% CD8$^+$ T cells (Figure 6D). Next, we used FH9 and FK10 tetramers labeled with different fluorophores to detect dual-staining T cell

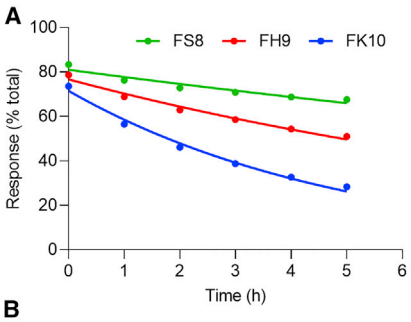

Peptide sequence	$t_{1/2}$ (h)
FS8: FLGKIWPS	16.92
FH9: FLGKIWPSH	7.98
FK10: FLGKIWPSHK	3.46

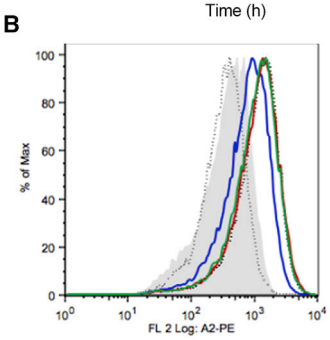

Peptide sequence	Net MFI (FL2 log)	FI
FS8: FLGKIWPS	1208	2.93
FH9: FLGKIWPSH	1266	3.07
FK10: FLGKIWPSHK	866	2.1
SL9: SLFNTVATL	1310	3.18
LM9: LPFDKTTVM (dotted line)	367	0.89
T2 only (shaded area)	412	

Figure 5. Stability of FH9 in HLA-A*02:01

(A) The half-life ($t_{1/2}$) of functionally folded FS8, FH9, and FK10 peptides loaded in HLA-A*02:01, as assessed by binding of soluble ILT2 to intact complexes over time. Responses shown are relative to total immobilized peptide-HLA complex, measured by surface plasmon resonance.

(B) T2 peptide binding assay: cell surface HLA-A2 expression was detected by staining T2 cells pulsed with HLA-A*02:01-binding peptides (FH9, FK10, and SL9) with anti-human HLA-A2-PE antibody, depicted by shift in median fluorescence (histogram, left; maximal response to peptide [100 μM], right). A non-HLA-A*02-binding peptide (influenza A nucleoprotein, LM9) was used as a negative control. Table shows net median fluorescence values (unstained cell value subtracted) and fluorescence index (FI; ratio of MFI with test peptide to control peptide). Data shown are representative of two experiments.

populations. We observed a mixed pattern of staining across the five subjects, with the majority of cells showing a separate FH9 or FK10 single-reactive population in four of the five tested individuals (Figure 6D). The detection of FH9 single-staining T cells indicates that reactivity to FH9 was not solely because of the presence of FK10-specific T cells that also recognize a shorter version of the cognate epitope. On the contrary, it suggests that some individuals made a specific response to an epitope that is largely presented during the intracellular eclipse phase.

To investigate this further, we assessed the functional avidity, also known as antigen sensitivity, of polyclonal T cells to FH9 and FK10 in all seven FK10 responders using titrated peptide concentrations in an *ex vivo* IFN-γ ELISpot assay. The median peptide concentration required to achieve half-maximal responses (EC_{50}) was 1,382 ng/mL for FH9 and 49 ng/mL for FK10 (Figure 6E). When taking into consideration the observation that the FH9 pHLA has a higher stability than the FK10 complex, these results suggested that circulating polyclonal T cells may be dominated by T cell clones with a stronger T cell receptor affinity for the 10-mer than the 9-mer. Alternatively, they could reflect more efficient priming through cross-presentation of FK10, which would be generated in productively infected cells.

FH9-specific T cells are able to eliminate HIV-infected targets during the intracellular eclipse phase

T cell functional avidity, as measured by the response to titrated cognate peptide, has been associated with antiviral potency (Almeida et al., 2007, 2009; Mothe et al., 2012). Under these experimental conditions, cell surface peptide-HLA (pHLA) density is controllable by exogenous loading of peptide onto HLA molecules, whereas *in vivo* it is influenced by multiple steps in the endogenous pathway, including the effects of HIV Nef on the trafficking of HLA class I molecules (Balamurugan et al., 2013; Ali et al., 2004; Chen et al., 2012). Therefore, functional avidity may not be sufficient to explain antiviral potency in all cases. We hypothesized that, despite their relatively low functional avidity, FH9-specific $CD8^+$ T cells would have potent antiviral activity because the early presentation of FH9 should protect it from Nef-mediated HLA class I downregulation. To test this, we performed a 6-h whole virus killing assay. Purified $CD4^+$ T cells from an HLA-A*02:01-positive HIV-naive donor were infected with HIV-GFP and cultured for 6 h with either bulk FH9 tetramer-sorted or FH9 tetramer-depleted $CD8^+$ T cells from the same five subjects (BCN01–05; Table S1). Given the low number of tetramer-positive cells obtained post-sort (median, 1,800; range, 365–11,000 cells), their potency could be evaluated only at low effector/target (E:T) ratios (range, 1:20–1:50). Elimination of infected cells by FH9-positive cells was detected by 6 h in all five subjects (range, 10%–39% for the four subjects in whom an E:T ratio of 1:20 was tested) and was reduced in all cases by depletion of this population (Figure 7A). Bulk $CD8^+$ T cells gave a marginally stronger response than sorted FH9-specific T cells in only one subject (L8154, 29% versus 25%), suggesting that intracellular eclipse phase killing was mediated predominantly, if not exclusively, by FH9-specific T cells in all five individuals.

We extended these results by generating FH9-specific short-term T cell lines (STCLs) from three CHI-ART subjects (OXF12, OXF20, and OXF21; Table S1) to enable assessment of killing at an E:T ratio of 1:1, again using HIV-GFP-infected HLA-A*02:01-positive $CD4^+$ T cells as targets. We extended the duration of this assay to 16 h to take advantage of the later expression of Nef (indicated by the emergence of GFP-positive cells; Figure 1B), and thus to determine the maximal elimination of infected cells during the intracellular eclipse phase. These STLCs eliminated up to 80% of Gag-positive cells by 16 h. To verify these results, half of the cultures were maintained for a total of 3 days, and the quantity of cell-free HIV p24 in culture supernatants was measured by ELISA. Reductions in p24 of 0.4–1.3 log10 pg/mL were observed in cultures with STLC

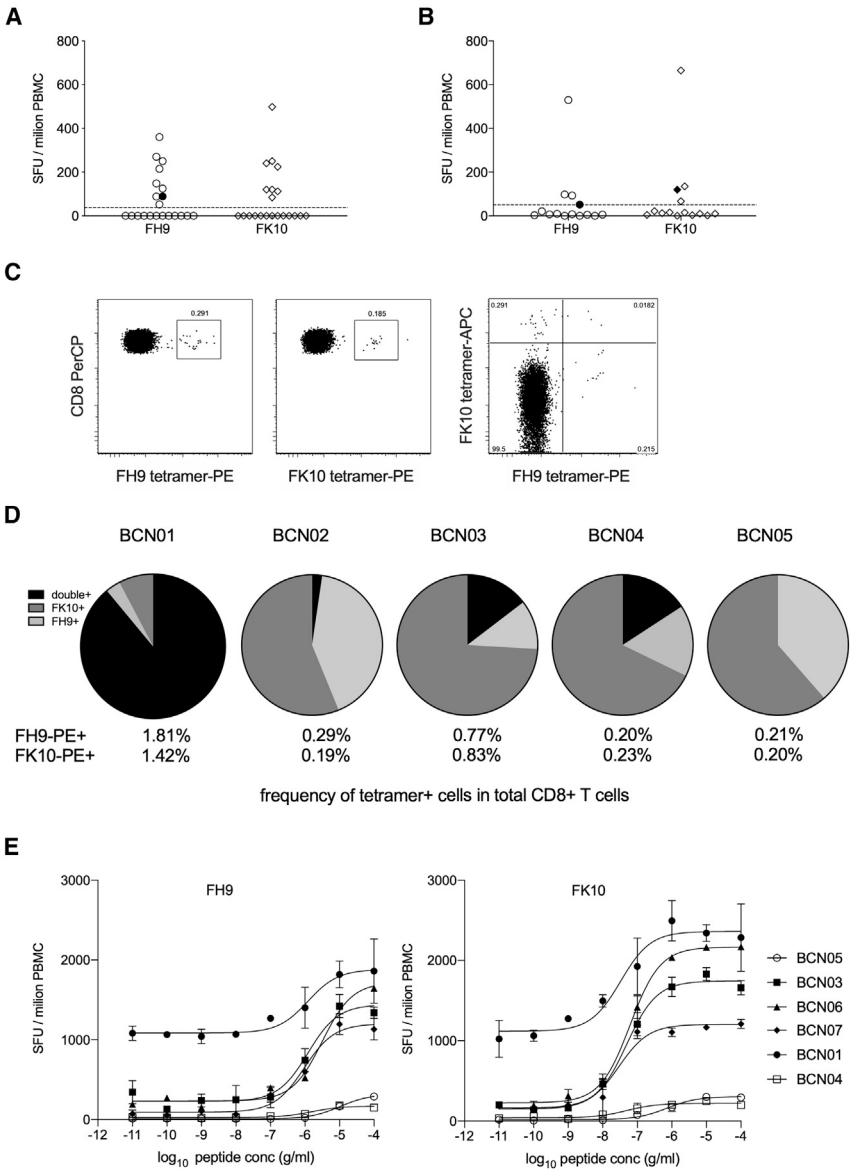

Figure 6. CD8⁺ T cell responses to FH9 in chronic infection are due to distinct T cell populations targeting FH9 alone or with cross-reactivity to FK10

(A and B) Frequency of FH9- and FK10-specific T cells determined in *ex vivo* IFN-γ ELISpot assays with PBMCs from (A) individuals treated with ART during acute infection (n = 21, PHI) or (B) chronic infection (n = 11, CHI-ART). Mock-stimulated values have been subtracted. Filled symbols indicate subjects with a response to either FH9 or FK10 but not both.

(C) Representative flow cytometry plot of *ex vivo* CD8⁺ T cells from an HIV controller (HIC), BCN02, showing FH9- and FK10 tetramer-staining cells, after gating on singlet live CD3⁺ cells.

(D) Co-staining with PE- and allophycocyanin (APC)-labeled tetramers demonstrates the presence of dual-reactive T cells in 4/5 known FK10 responders (2 non-controllers [NCs], 3 HICs). Single-reactive tetramer responses to FH9 were detected in all subjects (0.07%–0.2% CD8⁺ T cells).

(E) Functional avidity of FH9- and FK10-reactive T cells from 5 HIC and 2 NC subjects, determined by IFN-γ release in response to serial dilutions of peptide in *ex vivo* ELISpot assays. EC_{50} values were obtained by non-linear (least-squares) fit.

effectors, relative to HIV-GFP-infected CD4⁺ T cells alone (Figure 7B).

In summary, these data show that presentation of the HLA-A*02:01-restricted FH9 epitope during the intracellular eclipse phase was sufficient to trigger a potent antiviral response in the majority of subjects studied.

DISCUSSION

Presentation of virion-derived peptides early in the viral intracellular life cycle has been inferred from studies in SIV and HIV infection, in which killing of infected cells by CD8⁺ T cells was observed before *de novo* viral protein synthesis (Sacha et al., 2007a; Payne et al., 2010; Kløverpris et al., 2013 Buckheit et al., 2013). In human subjects, this phenomenon has been defined using CD8⁺ T cells from HICs who recognized viral epitopes presented by HLA-B*57/58 or B*27:05, all alleles that are known to be associated with viral containment. In the present study, we used short-term killing assays to show that elimination of infected CD4⁺ T cells during the intracellular eclipse phase of the viral life cycle can be triggered by early peptide presentation in the context of diverse HLA allotypes. We were able to identify virion-derived peptides from Gag SP2 within 6 h of infection, one of which is a 9-mer version (FH9) of a known HLA-A*02:01-restricted epitope that has not been described before. Finally, we show that the FH9 epitope is presented at sufficient levels to elicit potent CD8⁺ T cell cytolytic activity in the context of HLA-A*02:01, which is not considered to be a beneficial HLA class I allele. Collectively, our observations demonstrate that eclipse phase killing makes a significant contribution to the overall antiviral efficacy of CD8⁺ T cells *in vitro*. We speculate that this mechanism could contribute to virological control that has been reported in rare HIC individuals who lack favorable HLA alleles; however, proof would require analysis of a substantial number of HICs, given the multifactorial nature of HIV control (Mothe et al., 2011; Hancock et al., 2015).

Peptide elution and LC-MS/MS enabled us to demonstrate HIV peptide presentation in non-productively infected cells by a direct method, providing crucial evidence that complements the previous reports of early peptide presentation described above (Sacha et al., 2007a; Payne et al., 2010; Kløverpris et al., 2013; Buckheit et al., 2013). Our approach yielded three unique

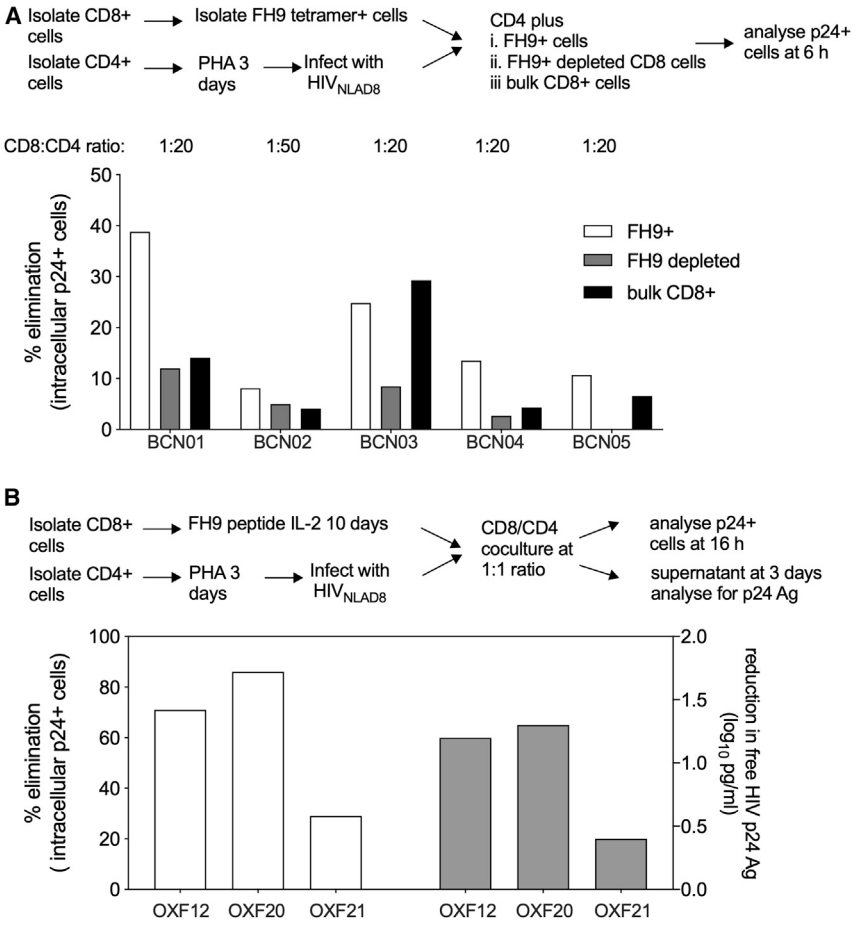

Figure 7. FH9-specific CD8$^+$ T cells are capable of eliminating infected cells during the intracellular eclipse phase

(A) Elimination of Gag p24-positive (HIV-GFP infected) CD4$^+$ T cells from an HIV-uninfected HLA-A*02:01 donor by FH9 tetramer-sorted CD8$^+$ T cells from the 2 NCs and 3 HICs after co-culture for 6 h post-infection. Effector/target ratios were determined by post-sort cell recovery. Antiviral activity was also assessed using bulk CD8$^+$ T cells and the FH9-depleted fraction from each individual.

(B) FH9-specific short-term cell lines from 3 CHI-ART individuals were tested for their capacity to eliminate autologous HIV-GFP superinfected CD4$^+$ T cells, as measured by intracellular p24 staining (left y axis) and quantification of p24 concentration in culture supernatants by ELISA (right y axis).

HIV peptides across three donors, two of which were truncated variants of a known HLA-A*02:01-restricted epitope in Gag SP2. Furthermore, we demonstrated that the 9-mer version of this epitope was presented almost exclusively during the intracellular eclipse phase, providing a mechanism for triggering killing of non-productively infected cells. The detection of unlabeled FH9 peptide 6 h post-infection, using stable isotope labeling of amino acids, provided an additional level of evidence that it was derived from incoming virions. The source of the identified peptide in Gag SP2 is of interest because SP2 is the second most conserved region of Gag after the capsid, yet very little is known about its biological function. It forms secondary RNA stem-loop structures and is a component of the *gag-pol* frameshift signal, which is critical for the production of the Pol polyprotein. Additionally, it is present in both *gag* and *pol* open reading frames. Mutations (e.g., P at position 7) can affect processing, RNA dimer stability, and infectivity (Hill et al., 2007). Mutations in Gag SP2 may affect nucleocapsid function, particularly in early stages of reverse transcription and integration, yet SP2 appears to play a minor role in viral infectivity (de Marco et al., 2012). CD8$^+$ T cell targeting of viral epitopes that cannot tolerate mutation is thought to play a significant role in spontaneous control of viremia (Miura et al., 2009; Brockman et al., 2010; Mothe et al., 2011; Hancock et al., 2015). Consistent with this notion, CD8$^+$ T cell responses to the Gag SP2 epitope, FK10 (Y9 variant), were found to be associated with delayed initiation of ART in an observational study (Streeck et al., 2014) and were also observed in an individual with spontaneous HIV control of 15 years' duration (Jessen et al., 2014). Although the extreme phenotype of the latter case was ascribed largely to the expression of HLA-B*57:01, a comprehensive analysis of >600 subjects from a South African chronic infection cohort showed that recognition of Gag SP2 peptides was associated with lower viral load setpoint (Mothe et al., 2011). Therefore, we conclude that SP2, and in particular the FH9 epitope, could be an important target for cytolytic T cells because of the high viral fitness cost of mutations in this region of *gag*, coupled with the relative insensitivity of FH9 to Nef-mediated HLA class I downregulation because of its early presentation.

Several studies have reported responses to FK10 in chronic and acute HIV infection, whereas data on the 9-mer variants are scarce. This raises the question of whether the 10-mer is preferentially presented post-transcriptionally, i.e., in productively infected cells. Alternatively, the studies based on 10-mer peptides FK10 (H9 or Y9 variant) may have detected, but not discriminated, responses targeting the 9-mer epitope. Indeed, it appears that only one study tested for recognition of length variants. This demonstrated lower functional avidity (higher EC_{50}) for the 9-mer (FY9) than FK10, which is in agreement with our results (Yu et al., 2002). Given that the 9-mer forms a more stable complex with HLA-A*02:01 than the 10-mer, these observations suggest that the higher functional avidity of T cell clones specific for the 10-mer may be because of a preponderance of TCRs that recognize pHLA complexes presenting the 10-mer in the naive repertoire (Sewell, 2012). The dominance of dual-reactive and FK10 single-reactive over FH9 single-reactive cells within tetramer staining CD8$^+$ T cell populations that we observed in this study supports this notion. However, confirmation would

require single-cell sorting and T cell receptor sequencing, which could not be conducted with the samples available. A further question is why FH9 single-reactive T cells were detectable in individuals with chronic infection, given its transient expression during the viral life cycle. We speculate that several mechanisms might account for this, such as preferential presentation of the FH9 peptide in lymphoid tissues, through virion transfer from dendritic cells (DCs) to T cells or differential processing of viral antigens in DCs, or specific characteristics of FH9 single-reactive T cell clones that confer a survival advantage (Pope and Haase, 2003; Steers et al., 2011). These hypotheses require formal testing.

A limitation of using mass spectrometry to interrogate the viral peptidome is its capacity to discriminate the small number of viral peptides from the vast number of self-peptides that makes up the majority of HLA ligands. Previously, we showed in productively HIV-infected $CD4^+$ T cells, either using a permissive cell line (C8166) or activated PBMCs from HIV-uninfected donors ($\sim 10^8$ cells per sample) cultured for several days, that HIV peptides accounted for 1.1% of HLA class I-associated peptides (75/7,000 peptides) (Ternette et al., 2016). Here, we identified three distinct HIV peptides 6 h post-infection, among a total of up to 3,000 HLA class I-associated peptides ($\sim$0.1%). It is possible that the mass spectrometry approach used here failed to detect other viral peptides for technical reasons. *In vivo*, the abundance of viral peptides on the cell surface is determined by multiple factors, such as susceptibility of viral proteins to proteolytic cleavage, transporter-associated protein activity, and editing of HLA class I-bound peptides by aminopeptidases. These processes may, in turn, be affected by the activation state of the cell (Monel et al., 2019). Nevertheless, our data indicate that mining the HLA class I peptidome for early presented peptides is feasible, despite the short window during which Gag from incoming virions is processed, and it can yield a different set of viral epitopes from those identified in productively infected cells. If elimination of HIV-infected cells prior to viral integration can help to interrupt the onset of viral replication and the formation of latent reservoirs, it will be important to determine whether these epitopes are suitable targets for vaccines and therapeutic interventions.

STAR★METHODS

Detailed methods are provided in the online version of this paper and include the following:

- KEY RESOURCES TABLE
- RESOURCE AVAILABILITY
  - Lead contact
  - Materials availability
  - Data and code availability
- EXPERIMENTAL MODEL AND SUBJECT DETAILS
  - Study subjects
  - Cell lines
- METHOD DETAILS
  - Production of HIV-GFP
  - HIV infection of primary CD4+ T cells
  - Detection of Gag proteins by SDS-PAGE and western blotting
  - Infected cell elimination assay
  - Isolation of HLA class I associated peptides
  - Generation of trypsin-digested cell lysates for p24 protein quantification by LC-MS/MS
  - LC-MS/MS analysis
  - Mass spectrometry data analysis
  - Stable isotope labeling by amino acids in cell culture (SILAC)
  - BIAcore analysis
  - T2 peptide binding assay
  - IFN-γ Elispot assay
  - HLA class I tetramer staining
- QUANTIFICATION AND STATISTICAL ANALYSIS

SUPPLEMENTAL INFORMATION

Supplemental information can be found online at https://doi.org/10.1016/j.celrep.2021.109103.

CONSORTIUM

Research in Viral Eradication of Reservoirs (RIVER) trial study group: Eric Sandström, Janet Darbyshire, Frank Post, Christopher Conlon, Jane Anderson, Mala Maini, Timothy Peto, Peter Sasieni, Veronica Miller, Ian Weller, Sarah Fidler, John Frater, Abdel Babiker, Wolfgang Stöhr, Sarah Pett, Lucy Dorrell, Matthew Pace, Natalia Olejniczak, Helen Brown, Nicola Robinson, Jakub Kopycinski, Hongbing Yang, Tomáš Hanke, Alison Crook, Steven Kaye, Myra McClure, Otto Erlwein, Andrew Lovell, Maryam Khan, Michelle Gabrielle, Rachel Bennett, Aminata Sy, Adam Gregory, Fleur Hudson, Charlotte Russell, Gemma Wood, Hanna Box, Cherry Kingsley, Katie Topping, Andrew Lever, Mark Wills, Axel Fun, Mikaila Bandara, Damian Kelly, Simon Collins, Alex Markham, Mary Rauchenberger, Yinka Sowunmi, Shaadi Shidfar, Dominic Hague, Mark Nelson, Maddalena Cerrone, Nadia Castrillo Martinez, Tristan Barber, Alexandra Schoolmeesters, Christine Weaver, Orla Thunder, Jane Rowlands, Christopher Higgs, Serge Fedele, Margherita Bracchi, Lervina Thomas, Peter Bourke, Nneka Nwokolo, Gaynor Lawrenson, Marzia Fiorino, Hinal Lukha, Sabine Kinloch-de Loes, Margaret Johnson, Alice Nightingale, Nnenna Ngwu, Patrick Byrne, Zoe Cuthbertson, Martin Jones, Tina Fernandez, Amanda Clarke, Martin Fisher, Rebecca Gleig, Vittorio Trevitt, Colin Fitzpatrick, Tanya Adams, Fiounnuala Finnerty, John Thornhill, Heather Lewis, Kristin Kuldanek, Julie Fox, Julianne Lwanga, Hiromi Uzu, Ming Lee, Simon Merle, Patrick O'Rourke, Isabel Jendrulek, Taras Zarko Flynn, Mark Taylor, Juan Manuel Tiraboschi, Tammy Murray.

ACKNOWLEDGMENTS

The authors would like to thank Emma Gostick, Immunocore Ltd, for reagent preparation. MS data acquisition was performed in the Target Discovery Institute Mass Spectrometry Laboratory run by Benedikt M. Kessler. This work was supported in part by UK National Institute for Health Research (NIHR) infrastructure through the National Institute for Health Research (NIHR) Biomedical Research Centres based at University of Oxford, Imperial College Healthcare NHS Trust and Imperial College London, University of Cambridge, and King's College London. The views expressed in this article are those of the authors and not necessarily those of the NHS, the NIHR, or the Department of Health. GSK provided the ChAdV63 vector used in the RIVER study. GlaxoSmithKline Biologicals SA provided the opportunity to review a preliminary version of this manuscript for factual accuracy, but the authors are solely responsible for final content and interpretation. This work was supported by the Australian Research Council (FT100100297 to J.M.), Australian National Health and Medical Research Council Project Grant (1121697 to J.M.), the European Union's Horizon 2020 Research and Innovation Programme (Grant Agreement No. 681137 to C.B.), and the UK Medical Research Council (G0502048 to L.D.).

AUTHOR CONTRIBUTIONS

Study design or conception: H.Y., C.B., N.T., and L.D. Methodology: H.Y., G.M.G., and A.K. Investigation: H.Y., A.L., S.C., A.C., D.B.L., W.S., and N.T. Resources: J.F., S.F., B.M., J.M., C.B., N.T., and L.D. Writing – Original Draft: H.Y., A.v.D., N.T., and L.D. Writing – Review & Editing: H.Y., A.L., G.G., A.K., S.F., B.M., J.M., C.B., N.T., and L.D. Visualization: H.Y., A.v.D., D.B.L., N.T., and L.D. Supervision: C.B., N.T., and L.D. Funding acquisition: J.F., S.F., J.M., C.B., N.T., and L.D.

DECLARATION OF INTERESTS

L.D. is an employee of Immunocore Ltd. A.K. and D.B.L. were previously employees of Immunocore Ltd.

Received: October 6, 2020
Revised: February 20, 2021
Accepted: April 16, 2021
Published: May 11, 2021

REFERENCES

Abrahams, M.-R., Joseph, S.B., Garrett, N., Tyers, L., Moeser, M., Archin, N., Council, O.D., Matten, D., Zhou, S., Doolabh, D., et al. (2019). The replication-competent HIV-1 latent reservoir is primarily established near the time of therapy initiation. Sci. Transl. Med. *11*, eaaw5589.

Ali, A., Lubong, R., Ng, H., Brooks, D.G., Zack, J.A., and Yang, O.O. (2004). Impacts of epitope expression kinetics and class I downregulation on the antiviral activity of human immunodeficiency virus type 1-specific cytotoxic T lymphocytes. J. Virol. *78*, 561–567.

Almeida, J.R., Price, D.A., Papagno, L., Arkoub, Z.A., Sauce, D., Bornstein, E., Asher, T.E., Samri, A., Schnuriger, A., Theodorou, I., et al. (2007). Superior control of HIV-1 replication by CD8+ T cells is reflected by their avidity, polyfunctionality, and clonal turnover. J. Exp. Med. *204*, 2473–2485.

Almeida, J.R., Sauce, D., Price, D.A., Papagno, L., Shin, S.Y., Moris, A., Larsen, M., Pancino, G., Douek, D.C., Autran, B., et al. (2009). Antigen sensitivity is a major determinant of CD8+ T-cell polyfunctionality and HIV-suppressive activity. Blood *113*, 6351–6360.

Althaus, C.L., and De Boer, R.J. (2011). Implications of CTL-mediated killing of HIV-infected cells during the non-productive stage of infection. PLoS ONE *6*, e16468.

Altman, J.D., Moss, P.A., Goulder, P.J., Barouch, D.H., McHeyzer-Williams, M.G., Bell, J.I., McMichael, A.J., and Davis, M.M. (1996). Phenotypic analysis of antigen-specific T lymphocytes. Science *274*, 94–96.

Balamurugan, A., Ali, A., Boucau, J., Le Gall, S., Ng, H.L., and Yang, O.O. (2013). HIV-1 Gag cytotoxic T lymphocyte epitopes vary in presentation kinetics relative to HLA class I downregulation. J. Virol. *87*, 8726–8734.

Betts, M.R., Nason, M.C., West, S.M., De Rosa, S.C., Migueles, S.A., Abraham, J., Lederman, M.M., Benito, J.M., Goepfert, P.A., Connors, M., et al. (2006). HIV nonprogressors preferentially maintain highly functional HIV-specific CD8+ T cells. Blood *107*, 4781–4789.

Brockman, M.A., Brumme, Z.L., Brumme, C.J., Miura, T., Sela, J., Rosato, P.C., Kadie, C.M., Carlson, J.M., Markle, T.J., Streeck, H., et al. (2010). Early selection in Gag by protective HLA alleles contributes to reduced HIV-1 replication capacity that may be largely compensated for in chronic infection. J. Virol. *84*, 11937–11949.

Bruner, K.M., Murray, A.J., Pollack, R.A., Soliman, M.G., Laskey, S.B., Capoferri, A.A., Lai, J., Strain, M.C., Lada, S.M., Hoh, R., et al. (2016). Defective proviruses rapidly accumulate during acute HIV-1 infection. Nat. Med. *22*, 1043–1049.

Buckheit, R.W., 3rd, Siliciano, R.F., and Blankson, J.N. (2013). Primary CD8+ T cells from elite suppressors effectively eliminate non-productively HIV-1 infected resting and activated CD4+ T cells. Retrovirology *10*, 68.

Bui, J.K., Sobolewski, M.D., Keele, B.F., Spindler, J., Musick, A., Wiegand, A., Luke, B.T., Shao, W., Hughes, S.H., Coffin, J.M., et al. (2017). Proviruses with identical sequences comprise a large fraction of the replication-competent HIV reservoir. PLoS Pathog. *13*, e1006283.

Chadwick, K.H. (1973). A molecular theory of cell survival. Phys Med Biol *18*, 78–87. https://doi.org/10.1088/0031-9155/18/1/007.

Chen, D.Y., Balamurugan, A., Ng, H.L., Cumberland, W.G., and Yang, O.O. (2012). Epitope targeting and viral inoculum are determinants of Nef-mediated immune evasion of HIV-1 from cytotoxic T lymphocytes. Blood *120*, 100–111.

Chomont, N., El-Far, M., Ancuta, P., Trautmann, L., Procopio, F.A., Yassine-Diab, B., Boucher, G., Boulassel, M.-R., Ghattas, G., Brenchley, J.M., et al. (2009). HIV reservoir size and persistence are driven by T cell survival and homeostatic proliferation. Nat. Med. *15*, 893–900.

Chun, T.W., Stuyver, L., Mizell, S.B., Ehler, L.A., Mican, J.A., Baseler, M., Lloyd, A.L., Nowak, M.A., and Fauci, A.S. (1997). Presence of an inducible HIV-1 latent reservoir during highly active antiretroviral therapy. Proc. Natl. Acad. Sci. USA *94*, 13193–13197.

de Marco, A., Heuser, A.-M., Glass, B., Kräusslich, H.-G., Müller, B., and Briggs, J.A.G. (2012). Role of the SP2 domain and its proteolytic cleavage in HIV-1 structural maturation and infectivity. J. Virol. *86*, 13708–13716.

Deeks, S.G., and Walker, B.D. (2007). Human immunodeficiency virus controllers: mechanisms of durable virus control in the absence of antiretroviral therapy. Immunity *27*, 406–416.

Doitsh, G., Cavrois, M., Lassen, K.G., Zepeda, O., Yang, Z., Santiago, M.L., Hebbeler, A.M., and Greene, W.C. (2010). Abortive HIV infection mediates CD4 T cell depletion and inflammation in human lymphoid tissue. Cell *143*, 789–801.

Emu, B., Sinclair, E., Hatano, H., Ferre, A., Shacklett, B., Martin, J.N., McCune, J.M., and Deeks, S.G. (2008). HLA class I-restricted T-cell responses may contribute to the control of human immunodeficiency virus infection, but such responses are not always necessary for long-term virus control. J. Virol. *82*, 5398–5407.

Fidler, S., Stöhr, W., Pace, M., Dorrell, L., Lever, A., Pett, S., Kinloch-de Loes, S., Fox, J., Clarke, A., Nelson, M., et al.; RIVER trial study group (2020). Antiretroviral therapy alone versus antiretroviral therapy with a kick and kill approach, on measures of the HIV reservoir in participants with recent HIV infection (the RIVER trial): a phase 2, randomised trial. Lancet *395*, 888–898.

Finzi, D., Hermankova, M., Pierson, T., Carruth, L.M., Buck, C., Chaisson, R.E., Quinn, T.C., Chadwick, K., Margolick, J., Brookmeyer, R., et al. (1997). Identification of a reservoir for HIV-1 in patients on highly active antiretroviral therapy. Science *278*, 1295–1300.

Freed, E.O., Englund, G., and Martin, M.A. (1995). Role of the basic domain of human immunodeficiency virus type 1 matrix in macrophage infection. J. Virol. *69*, 3949–3954.

Garboczi, D.N., Hung, D.T., and Wiley, D.C. (1992). HLA-A2-peptide complexes: refolding and crystallization of molecules expressed in Escherichia coli and complexed with single antigenic peptides. Proc. Natl. Acad. Sci. USA *89*, 3429–3433.

Gibbs, J.S., Regier, D.A., and Desrosiers, R.C. (1994). Construction and in vitro properties of HIV-1 mutants with deletions in "nonessential" genes. AIDS Res. Hum. Retroviruses *10*, 343–350.

Goulder, P., and Deeks, S.G. (2018). HIV control: Is getting there the same as staying there? PLoS Pathog. *14*, e1007222.

Graf, E.H., Mexas, A.M., Yu, J.J., Shaheen, F., Liszewski, M.K., Di Mascio, M., Migueles, S.A., Connors, M., and O'Doherty, U. (2011). Elite suppressors harbor low levels of integrated HIV DNA and high levels of 2-LTR circular HIV DNA compared to HIV+ patients on and off HAART. PLoS Pathog. *7*, e1001300.

Hancock, G., Yang, H., Yorke, E., Wainwright, E., Bourne, V., Frisbee, A., Payne, T.L., Berrong, M., Ferrari, G., Chopera, D., et al. (2015). Identification of effective subdominant anti-HIV-1 CD8+ T cells within entire post-infection and post-vaccination immune responses. PLoS Pathog. *11*, e1004658.

Hancock, G., Morón-López, S., Kopycinski, J., Puertas, M.C., Giannoulatou, E., Rose, A., Salgado, M., Hayton, E.J., Crook, A., Morgan, C., et al. (2017).

Evaluation of the immunogenicity and impact on the latent HIV-1 reservoir of a conserved region vaccine, MVA.HIVconsv, in antiretroviral therapy-treated subjects. J. Int. AIDS Soc. *20*, 21171.

Hill, M.K., Bellamy-McIntyre, A., Vella, L.J., Campbell, S.M., Marshall, J.A., Tachedjian, G., and Mak, J. (2007). Alteration of the proline at position 7 of the HIV-1 spacer peptide p1 suppresses viral infectivity in a strain dependent manner. Curr. HIV Res. *5*, 69–78.

Jessen, H., Allen, T.M., and Streeck, H. (2014). How a single patient influenced HIV research—15-year follow-up. N. Engl. J. Med. *370*, 682–683.

Kløverpris, H.N., Payne, R.P., Sacha, J.B., Rasaiyaah, J.T., Chen, F., Takiguchi, M., Yang, O.O., Towers, G.J., Goulder, P., and Prado, J.G. (2013). Early antigen presentation of protective HIV-1 KF11Gag and KK10Gag epitopes from incoming viral particles facilitates rapid recognition of infected cells by specific CD8+ T cells. J. Virol. *87*, 2628–2638.

Kwaa, A.K.R., Garliss, C.C., Ritter, K.D., Laird, G.M., and Blankson, J.N. (2020). Elite suppressors have low frequencies of intact HIV-1 proviral DNA. AIDS *34*, 641–643.

Lambotte, O., Boufassa, F., Madec, Y., Nguyen, A., Goujard, C., Meyer, L., Rouzioux, C., Venet, A., and Delfraissy, J.F.; SEROCO-HEMOCO Study Group (2005). HIV controllers: a homogeneous group of HIV-1-infected patients with spontaneous control of viral replication. Clin. Infect. Dis. *41*, 1053–1056.

Llano, A., Cedeño, S., Silva Arrieta, S., and Brander, C. (2019). The 2019 Optimal HIV CTL epitopes update: Growing diversity in epitope length and HLA restriction. In HIV Molecular Immunology 2019, K. Yusim, B. Korber, C. Brander, D. Barouch, R. de Boer, B. Haynes, R. Koup, J. Moore, and B. Walker, eds. (Theoretical Biology and Biophysics Group, Los Alamos National Laboratory).

Miura, T., Brockman, M.A., Schneidewind, A., Lobritz, M., Pereyra, F., Rathod, A., Block, B.L., Brumme, Z.L., Brumme, C.J., Baker, B., et al. (2009). HLA-B57/B*5801 human immunodeficiency virus type 1 elite controllers select for rare gag variants associated with reduced viral replication capacity and strong cytotoxic T-lymphocyte [corrected] recognition. J. Virol. *83*, 2743–2755.

Monel, B., McKeon, A., Lamothe-Molina, P., Jani, P., Boucau, J., Pacheco, Y., Jones, R.B., Le Gall, S., and Walker, B.D. (2019). HIV Controllers Exhibit Effective $CD8^+$ T Cell Recognition of HIV-1-Infected Non-activated $CD4^+$ T Cells. Cell Rep. *27*, 142–153.e4.

Mothe, B., Llano, A., Ibarrondo, J., Daniels, M., Miranda, C., Zamarreño, J., Bach, V., Zuniga, R., Pérez-Álvarez, S., Berger, C.T., et al. (2011). Definition of the viral targets of protective HIV-1-specific T cell responses. J. Transl. Med. *9*, 208.

Mothe, B., Llano, A., Ibarrondo, J., Zamarreño, J., Schiaulini, M., Miranda, C., Ruiz-Riol, M., Berger, C.T., Herrero, M.J., Palou, E., et al. (2012). CTL responses of high functional avidity and broad variant cross-reactivity are associated with HIV control. PLoS ONE *7*, e29717.

Nelson, P.W., Mittler, J.E., and Perelson, A.S. (2001). Effect of drug efficacy and the eclipse phase of the viral life cycle on estimates of HIV viral dynamic parameters. J. Acquir. Immune Defic. Syndr. *26*, 405–412.

Partridge, T., Nicastri, A., Kliszczak, A.E., Yindom, L.-M., Kessler, B.M., Ternette, N., and Borrow, P. (2018). Discrimination Between Human Leukocyte Antigen Class I-Bound and Co-Purified HIV-Derived Peptides in Immunopeptidomics Workflows. Front. Immunol. *9*, 912.

Payne, R.P., Kløverpris, H., Sacha, J.B., Brumme, Z., Brumme, C., Buus, S., Sims, S., Hickling, S., Riddell, L., Chen, F., et al. (2010). Efficacious early antiviral activity of HIV Gag- and Pol-specific HLA-B 2705-restricted CD8+ T cells. J. Virol. *84*, 10543–10557.

Pereyra, F., Addo, M.M., Kaufmann, D.E., Liu, Y., Miura, T., Rathod, A., Baker, B., Trocha, A., Rosenberg, R., Mackey, E., et al. (2008). Genetic and immunologic heterogeneity among persons who control HIV infection in the absence of therapy. J. Infect. Dis. *197*, 563–571.

Pereyra, F., Heckerman, D., Carlson, J.M., Kadie, C., Soghoian, D.Z., Karel, D., Goldenthal, A., Davis, O.B., DeZiel, C.E., Lin, T., et al. (2014). HIV control is mediated in part by CD8+ T-cell targeting of specific epitopes. J. Virol. *88*, 12937–12948.

Pollack, R.A., Jones, R.B., Pertea, M., Bruner, K.M., Martin, A.R., Thomas, A.S., Capoferri, A.A., Beg, S.A., Huang, S.-H., Karandish, S., et al. (2017). Defective HIV-1 Proviruses Are Expressed and Can Be Recognized by Cytotoxic T Lymphocytes, which Shape the Proviral Landscape. Cell Host Microbe *21*, 494–506.e4.

Pope, M., and Haase, A.T. (2003). Transmission, acute HIV-1 infection and the quest for strategies to prevent infection. Nat. Med. *9*, 847–852.

Purcell, A.W., Ramarathinam, S.H., and Ternette, N. (2019). Mass spectrometry-based identification of MHC-bound peptides for immunopeptidomics. Nat. Protoc. *14*, 1687–1707.

Reeves, D.B., Duke, E.R., Wagner, T.A., Palmer, S.E., Spivak, A.M., and Schiffer, J.T. (2018). A majority of HIV persistence during antiretroviral therapy is due to infected cell proliferation. Nat. Commun. *9*, 4811.

Sacha, J.B., Chung, C., Rakasz, E.G., Spencer, S.P., Jonas, A.K., Bean, A.T., Lee, W., Burwitz, B.J., Stephany, J.J., Loffredo, J.T., et al. (2007a). Gag-specific CD8+ T lymphocytes recognize infected cells before AIDS-virus integration and viral protein expression. J. Immunol. *178*, 2746–2754.

Sacha, J.B., Chung, C., Reed, J., Jonas, A.K., Bean, A.T., Spencer, S.P., Lee, W., Vojnov, L., Rudersdorf, R., Friedrich, T.C., et al. (2007b). Pol-specific CD8+ T cells recognize simian immunodeficiency virus-infected cells prior to Nef-mediated major histocompatibility complex class I downregulation. J. Virol. *81*, 11703–11712.

Salter, R.D., Howell, D.N., and Cresswell, P. (1985). Genes regulating HLA class I antigen expression in T-B lymphoblast hybrids. Immunogenetics *21*, 235–246.

Sewell, A.K. (2012). Why must T cells be cross-reactive? Nat. Rev. Immunol. *12*, 669–677.

Shan, L., Deng, K., Shroff, N.S., Durand, C.M., Rabi, S.A., Yang, H.C., Zhang, H., Margolick, J.B., Blankson, J.N., and Siliciano, R.F. (2012). Stimulation of HIV-1-specific cytolytic T lymphocytes facilitates elimination of latent viral reservoir after virus reactivation. Immunity *36*, 491–501.

Shan, L., Deng, K., Gao, H., Xing, S., Capoferri, A.A., Durand, C.M., Rabi, S.A., Laird, G.M., Kim, M., Hosmane, N.N., et al. (2017). Transcriptional Reprogramming during Effector-to-Memory Transition Renders $CD4^+$ T Cells Permissive for Latent HIV-1 Infection. Immunity *47*, 766–775.e3.

Steers, N.J., Currier, J.R., Kijak, G.H., di Targiani, R.C., Saxena, A., Marovich, M.A., Kim, J.H., Michael, N.L., Alving, C.R., and Rao, M. (2011). Cell type-specific proteasomal processing of HIV-1 Gag-p24 results in an altered epitope repertoire. J. Virol. *85*, 1541–1553.

Streeck, H., Jolin, J.S., Qi, Y., Yassine-Diab, B., Johnson, R.C., Kwon, D.S., Addo, M.M., Brumme, C., Routy, J.-P., Little, S., et al. (2009). Human immunodeficiency virus type 1-specific CD8+ T-cell responses during primary infection are major determinants of the viral set point and loss of CD4+ T cells. J. Virol. *83*, 7641–7648.

Streeck, H., Lu, R., Beckwith, N., Milazzo, M., Liu, M., Routy, J.-P., Little, S., Jessen, H., Kelleher, A.D., Hecht, F., et al. (2014). Emergence of individual HIV-specific CD8 T cell responses during primary HIV-1 infection can determine long-term disease outcome. J. Virol. *88*, 12793–12801.

Ternette, N., Block, P.D., Sánchez-Bernabéu, Á., Borthwick, N., Pappalardo, E., Abdul-Jawad, S., Ondondo, B., Charles, P.D., Dorrell, L., Kessler, B.M., and Hanke, T. (2015). Early kinetics of the HLA class I-associated peptidome of MVA.HIVconsv-infected cells. J. Virol. *89*, 5760–5771.

Ternette, N., Yang, H., Partridge, T., Llano, A., Cedeño, S., Fischer, R., Charles, P.D., Dudek, N.L., Mothe, B., Crespo, M., et al. (2016). Defining the HLA class I-associated viral antigen repertoire from HIV-1-infected human cells. Eur. J. Immunol. *46*, 60–69.

Trautmann, L., Mbitikon-Kobo, F.-M., Goulet, J.-P., Peretz, Y., Shi, Y., Van Grevenynghe, J., Procopio, F.A., Boulassel, M.R., Routy, J.-P., Chomont, N., et al. (2012). Profound metabolic, functional, and cytolytic differences characterize HIV-specific CD8 T cells in primary and chronic HIV infection. Blood *120*, 3466–3477.

Yang, H., Wu, H., Hancock, G., Clutton, G., Sande, N., Xu, X., Yan, H., Huang, X., Angus, B., Kuldanek, K., et al. (2012). Antiviral inhibitory capacity of CD8+

T cells predicts the rate of CD4+ T-cell decline in HIV-1 infection. J. Infect. Dis. *206*, 552–561.

Yang, H., Yorke, E., Hancock, G., Clutton, G., Sande, N., Angus, B., Smyth, R., Mak, J., and Dorrell, L. (2013). Improved quantification of HIV-1-infected CD4+ T cells using an optimised method of intracellular HIV-1 gag p24 antigen detection. J. Immunol. Methods *391*, 174–178.

Yu, X.G., Shang, H., Addo, M.M., Eldridge, R.L., Phillips, M.N., Feeney, M.E., Strick, D., Brander, C., Goulder, P.J.R., Rosenberg, E.S., et al.; HIV Study Collaboration (2002). Important contribution of p15 Gag-specific responses to the total Gag-specific CTL responses. AIDS *16*, 321–328.

Zack, J.A., Kim, S.G., and Vatakis, D.N. (2013). HIV restriction in quiescent $CD4^+$ T cells. Retrovirology *10*, 37.

STAR★METHODS

KEY RESOURCES TABLE

REAGENT or RESOURCE	SOURCE	IDENTIFIER
Antibodies		
HLA-A2 PE, clone BB7.2	Biolegend	Cat # 343305; RRID:AB_1877228
Anti-human p24 KC57 FITC, clone KC57	Beckman Coulter	Cat # 6604665
Anti-human CD3 APC Cy7, clone SK7	BD Biosciences	Cat # 557832; RRID:AB_396890
Anti-human CD4 PerCP, clone SK3	BD Biosciences	Cat # 566924
Anti-human CD8 APC, clone RPA-T8	BD Biosciences	Cat # 561953' RRID:AB_10896290
Anti-human p24, clone 39/5.4A	Abcam	Cat # ab9071; RRID:AB_306981
Donkey anti-mouse IgG AlexaFluor 680, polyclonal	Abcam	Cat # ab175774
Rabbit anti-human β-tubulin, polyclonal	Abcam	Cat # ab6046; RRID:AB_2210370
Donkey anti-rabbit IgG AlexaFluor 488, polyclonal	Abcam	Cat # ab150065; RRID:AB_2860569
Anti-pan HLA class I, W6/32	ATCC	HB-95; RRID:CVCL_7872
Recombinant virus		
NLAD8 EGFP IRES_Nef	Prof. Johnson Mak, Griffith University	N/A
Biological samples		
PBMC samples from HIV-naive donors	NHS Blood & Transplant Service	https://www.nhsbt.nhs.uk/
PBMC samples from HIV-positive donors	University of Oxford; Irsicaixa AIDS Research Institute; MRC Clinical Trials Unit	N/A
Chemicals, peptides, and recombinant proteins		
Phytohaemagglutinin (PHA)	SIGMA Aldrich	Cat # L1668
Zidovudine	NIH AIDS Reagent Program	Cat # ARP-3485
Raltegravir	NIH AIDS Reagent Program	Cat # ARP-11680
IRDye 800CW Donkey anti-rabbit IgG	Li-Cor	Cat # P/N 925-32213; RRID:AB_2715510
Live/Dead fixable stain	Invitrogen	Cat # L34957
HIV Gag peptides	Genscript	https://www.genscript.com
Streptavidin-PE	SIGMA Aldrich	Cat # 42250-1ML
Streptavidin-APC	ThermoFisher Scientific	Cat # SA1005
HLA-A*02:01 Gag tetramers	NIH Tetramer Core Facility	https://tetramer.yerkes.emory.edu/
Heavy arginine, R10	Cambridge Isotope Laboratories	CNLM-539-H-PK
Heavy lysine, K4	Cambridge Isotope Laboratories	DLM-2640-PK
Critical commercial assays		
CD8 microbeads	Miltenyi Biotec	Cat # 130-045-201; RRID:AB_2889920
Human IFN-γ ELISpot kit	Mabtech	Cat # 3420-2H
Experimental models: Cell lines		
T2 (174xCEM.T2)	ATCC	https://www.lgcstandards-atcc.org/?geo_country=gb
T0 (721.174 and CEM.T0)	Prof. Andrew Sewell, University of Cardiff	N/A
Software and algorithms		
FlowJo v9	Becton Dickinson & Company	https://www.flowjo.com/
Graphpad Prism v8	GraphPad Software	https://www.graphpad.com/
Peaks 7.0	Bioinformatics Solutions	https://www.bioinfor.com/

RESOURCE AVAILABILITY

Lead contact

Further information and requests for resources and reagents should be directed to and will be fulfilled by the Lead Contact, Dr Hongbing Yang (hongbing.yang@ndm.ox.ac.uk). For queries relating to the mass spectrometry data please contact Prof Nicola Ternette (nicola.ternette@ndm.ox.ac.uk).

Materials availability

This study did not generate new unique reagents.

Data and code availability

This study did not generate any unique datasets or code.

EXPERIMENTAL MODEL AND SUBJECT DETAILS

Study subjects

PBMC from HIV-naive HLA-A*02:01-positive donors were isolated from buffy coats supplied by the NHS Blood & Transplant Service, Bristol, UK. PBMC were obtained from subjects from the following cohorts: Oxford (OXF) - chronic HIV infection, either ART-naive (CHI) or under long-term ART (CHI-ART); Barcelona (BCN) - chronic infection and ART-naive; PHI - RIVER trial participants. The latter had initiated ART within 4 weeks of confirmed primary HIV infection, which was defined using criteria described in (Fidler et al., 2020). They were randomized at Week 24 to receive a 'kick and kill' intervention in addition to ART or to continue ART alone and samples for the present study were obtained from the post-randomization Week 16 time-point. Written informed consent and ethical approval were obtained in all cases (UK Research Ethics Committee Refs: 08/H0607/51, 19/SW/0179, 10/H0604/95, 14/SC/1372 and the Institutional Review Board of the Hospital Germans Trias i Pujol (Ref EO-09-042).

Cell lines

T0 cells, a hybridoma of 721.174 and CEM.T0 cells, were kindly provided by Prof. Andrew Sewell, Cardiff University (Salter et al., 1985). T2 cells (174xCEM.T2) were obtained from American Type Culture Collection (ATCC) and were cultured in RPMI media supplemented with 10% fetal calf serum (FCS), 1% (v/v) penicillin/streptomycin and 2mM L-glutamine (R10 medium). Cell surface HLA-A2 expression after exogenous peptide loading was confirmed by staining with anti-HLA-A2 PE antibody (clone BB7.2, BioLegend).

METHOD DETAILS

Production of HIV-GFP

The EGFP-expressing R5-tropic HIV-1 isolate, NLAD8 EGFP IRES_Nef, was used to infect CD4+ T cells. A proviral clone was constructed from a pNL43 derivative, pDRNL43, which was modified to express a pNLAD8 envelope and EGFP (Gibbs et al., 1994; Freed et al., 1995). An ECMV IRES sequence was introduced to enable expression of full-length Nef. Viral stocks were prepared by transfection of 293T cells with polyethylenimine. After 36 hours, virus-containing supernatant was harvested, filtered, and frozen at −80°C.

HIV infection of primary CD4+ T cells

Purified CD4+ T cells were stimulated with PHA (5 μg/ml) in R10 medium for 72 hours, then washed and spinoculated with HIV-GFP at 2000 rpm, 27°C for 2 hours at an MOI of 0.01. In selected experiments, zidovudine (5 μM) or raltegravir (1 μM), both from NIH AIDS Reagent program were added immediately after infection.

Detection of Gag proteins by SDS-PAGE and western blotting

HIV-GFP-infected CD4+ T cells were washed with PBS, lysed, and centrifuged at 13000 rpm at 40°C. The supernatant was harvested and cytosolic proteins were reduced with 50 mM dithiothreitol (DTT, Merck) at 95°C for 15 minutes. Samples were analyzed on a NuPAGE Tris-acetate 4%–12% gel (Invitrogen, Thermo Fisher Scientific). β-tubulin (1 μg, Sigma) was included as a loading control and molecular weight was determined using Odyssey® Prestained Molecular Weight Marker (10 to 250 kDa, LI-COR). Proteins were blotted onto a nitrocellulose membrane (Merck Millipore) using Trans-Blot SD. Semi-Dry Transfer Cell (Bio-Rad Laboratories) at 200 mA for 80 minutes. Membranes were blocked (Odyssey Blocking buffer, LI-COR) for 1 hour, then stained with a 1/1000 dilution of mouse anti-human p24 monoclonal antibody (Abcam) in Odyssey Blocking buffer for 60 minutes at room temperature (RT). Membranes were washed in PBS containing 0.1% Tween-20, then stained with a 1/10,000 dilution of donkey anti-mouse IgG AlexaFluor 680 secondary antibody (LI-COR) for 30 minutes at RT and protected from light. After further wash steps, immunoblots were scanned using the Odyssey Infrared Imaging System and the intensity of the bands was calculated. To visualize β-tubulin, blots were first stained with a 1/1000 dilution of rabbit anti-human β-tubulin (Abcam) followed by a 1/10,000 dilution of donkey anti-rabbit IgG IRDye 800CW (LI-COR).

Infected cell elimination assay

Quantification of infected cell elimination was performed as previously described (Yang et al., 2012, 2013). Assays were performed on cryopreserved cells that had been thawed and rested for at least 2 hours prior to use. CD4+ and CD8+ T cell subsets were isolated by magnetic bead selection or depletion following the manufacturer's instructions (MACS, Miltenyi). In selected experiments, FH9-specific short-term CD8+ T cell lines were generated by stimulating PBMC from CHI donors with FH9 peptide (4 μg/ml) followed by culture in IL-7 (25ng/ml), IL-2 (1.8×10^3 units/ml) and 10% human serum for 10 days. HIV-GFP-infected CD4+ T cells (5×10^4) were cultured in triplicate in R10 with interleukin 2 (20 IU/mL) in 96-well round-bottomed plates, alone or together with autologous unstimulated *ex vivo* CD8+ T cells, obtained by positive bead selection of PBMCs from a second freshly thawed vial. CD8+ and CD4+ T cells were co-cultured for durations ranging from 2-96 hours at a CD8+/CD4+ ratio of 1:1. On the day of harvest, cells were stained first with Aqua Live/Dead Fixable stain (Invitrogen), fixed with 1% paraformaldehyde/20 μg/mL lysolecithin at RT, permeabilized with cold 50% methanol followed by 0.1% Nonidet P-40, and finally stained with p24 antibody (KC-57-FITC; Beckman Coulter) and antibodies to CD3, CD4, and CD8 (conjugated to APC-Cy7, PerCP, and APC, respectively; BD Biosciences). Samples were acquired on a CyAn ADP Analyzer flow cytometer (Beckman Coulter). Data were analyzed using FlowJo software v9. Infected cell elimination was expressed as a percentage and determined as follows: [(fraction of p24 + cells in CD4 + T cells cultured alone)–(fraction of p24 + in CD4+ T cells cultured with CD8+ cells)]/(fraction of p24 + cells in CD4 + T cells cultured alone) × 100. In selected experiments, HIV p24 Ag was quantified in culture supernatants by ELISA, as described previously (Yang et al., 2013).

Isolation of HLA class I associated peptides

Peptide-MHC class I complexes were captured from cleared cell lysates by protein A resin coupled to W6/32 antibody (ATCC HB-95) as described previously (Ternette et al., 2015). Complexes were washed with 50mM Tris buffer pH 8.0 with 150 nM NaCl, then 450 mM NaCl, and finally without salt. Complexes were eluted with 10% acetic acid. Dried MHC components were resuspended in loading buffer (1% acetonitrile, 1% triflouroacetic acid in water), loaded onto a 4.6 × 50mm ProSwift RP-1S column (ThermoFisher Scientific), and eluted using a 500μl/min flow rate over 10 minutes from 2%–35% Buffer B (0.1% formic acid in acetonitrile) in Buffer A (0.1% formic acid in water) using an Ultimate 3000 HPLC system (ThermoFischer Scientific).

Generation of trypsin-digested cell lysates for p24 protein quantification by LC-MS/MS

Cell lysates were generated by incubation in lysis buffer (0.5% IGEPAL®, 150 mM sodium chloride, 50 mM Tris, pH 8.0) for 30 min on ice. Lysates were cleared by centrifugation first at 500 g for 5 min to remove nuclei and then at 30,000 for 30 min to remove insoluble material. Lysates were incubated with a final concentration of 10 mM dithiothreitol for 15 min in order to reduce cysteine disulphide bonds followed by incubation with a final concentration of 40 mM iodoacetamine for cysteine alkylation. An equivalent of 10 - 20 μg total protein material as determined by BCA protein assay (Thermo Scientific) and proteins were separated at constant voltage (200V) for 1 hour. Gels were stained using InstantBlue (Expedeon) and gel bands corresponding to the mass of p24 were excised and cut into 1 mm^2 pieces. After destaining in 50% methanol, 5% acetic acid in water, gel pieces were dehydrated using repeated treatment with acetonitrile. A final amount of 200 ng trypsin was added in 50 mM ammonium bicarbonate and digestion was carried out overnight at 37°C. Tryptic peptides were eluted from the gel using elution buffer (50% acetonitrile, 0.1% triflouroacetic acid in water), dried and resuspended in loading buffer for LC-MS/MS analysis.

LC-MS/MS analysis

Samples were analyzed on either a TripleTOF 5600 system (Sciex, HLA-peptide samples) or a Q Exactive (Thermo Scientific, trypsin digested peptide material). TripleTOF 5600: Peptides were separated on an Ekspert nanoLC400 cHiPLC system (Eksigent), supplemented with a 15 cm x 75 μm ChromXP C18-CL, 3 μm particle size by application of a linear gradient from 8% to 35% buffer B in buffer A at a flow rate of 300 nl/min for 60 min. Peptides were introduced by an electrospray source. Collision-induced dissociation was induced on the 30 most abundant ions per full MS scan using ramped collision energy and a unit quadrupole isolation width of 0.7 amu. All fragmented precursor ions were actively excluded from repeated selection for 15 s. Q Exactive: Peptides were separated on an Ultimate 3000 RSLCnano System utilizing a PepMap C18 column, 2 μm particle size, 75 μm x 50 cm Thermo Scientific). Peptides were introduced into the mass spectrometer using an EASY-Spray™ nano source at a flowrate of 250 nl/min. Collision-induced dissociation was induced on the 15 most abundant ions per full MS scan (70,000 resolution) using a collision energy level of 28%, and a quadrupole isolation width of 1.6 amu. Precursor ions were allowed to accumulate for 128 ms, and fragment spectra were acquired at a resolution of 17,500. All fragmented precursor ions were actively excluded from repeated selection for 27 s.

Mass spectrometry data analysis

Raw data were analyzed using Peaks 7.0 software (Bioinformatics Solutions) using a precursor mass tolerance of 30 ppm, and a fragment mass tolerance of 0.05 Da. Sequence interpretation of MS2 spectra were performed using a database containing all annotated human SwissProt entries and all annotated protein coding regions from pDRNL43 and pDRNLAD8 (total of 21714 entries). The false discovery rate was determined by decoy database searches and was below 2% for all samples. Quantitative analyses were performed using Progenesis LC-MS QI v3.0 (Waters), and direct interrogation of the instrument data files using Analyst v1.6 (Sciex).

Stable isotope labeling by amino acids in cell culture (SILAC)

T0 cells were either cultured in RPMI-1640 medium supplemented with 10% FCS (RPMI-10) or RPMI medium lacking arginine and lysine supplemented with 10% FCS, heavy arginine (R10) (Cambridge Isotope laboratories, product number CNLM-539-H-PK; 13C6 99%; 15N4, 99%) and heavy lysine (K4) (Cambridge Isotope laboratories, product number DLM-2640-PK; 4,4,5,5-D4, 96%–98%). Cells were infected with HIV-GFP at an MOI of 0.01. At given time points post infections, cells were pelleted at 300 g for 5 min, washed once with PBS and frozen at −20°C until processing.

BIAcore analysis

HLA-A*02:01 and β2-microglobulin were produced as *E. coli* inclusion bodies and refolded in the presence of the peptide of interest to produce soluble peptide-HLA complexes, and similarly, ILT2 was refolded and purified from *E. coli* inclusion bodies, as previously described (Garboczi et al., 1992). Purified HLA-peptide complexes were subjected to SPR analysis using either a BIAcore™ T200 system. Briefly, biotinylated cognate pHLAs were immobilized onto a streptavidin-coupled CM5 sensor chip. The first flow cell was loaded with free biotin alone to act as a control surface. All measurements were performed at 25°C in Dulbecco's PBS buffer (Sigma-Aldrich, UK) containing P20 Surfactant (0.005%) at a flow rate of 10 μl/min. pHLA stability was measured by the binding of soluble Ig-like transcript 2 receptor (ILT2) (1 μM) at time zero and at one hour intervals over the following 5 hours. t1/2 values were calculated assuming Langmuir binding and data were analyzed using a 1:1 binding model (GraphPad Prism v8.3.0).

T2 peptide binding assay

T2 cells were resuspended in R0 and pulsed with control or test peptides (100 μM final concentration) for 3 hours at 37°C, then stained with anti-human HLA-A2-PE antibody (clone BB7.2, BioLegend) and analyzed by flow cytometry. Net median fluorescence intensity (MFI) was determined from the MFI detected in HLA-A2-stained cells after subtraction of MFI value for unstained cells. The fluorescence index for each peptide was calculated from the ratio of net MFI for the control or test peptide to net MFI for unpulsed cells. The HIV Gag p17 peptide, SLFNTVATL, was used as a positive control. An HLA-B7-restricted peptide from influenza A nucleoprotein (LPFDKTTVM) was used as a negative control.

IFN-γ Elispot assay

IFN-γ-detecting enzyme-linked immunoabsorbent spot (ELISpot) assays were performed as described previously, using the IFN-γ Mabtech kit in accordance with manufacturer's instructions. In brief, PBMC (1-2 × 10^5/well) were stimulated overnight with Gag p1 peptides (2 μg/ml final concentration; Genscript) in triplicate. Medium plus 0.45% DMSO only was used as the negative control in quadruplicate wells, and PHA (1 μg/mL) and a CEF peptide pool (2 μg/mL) consisting of 23 previously defined human CD8+ T cell epitopes from cytomegalovirus, Epstein–Barr virus and influenza virus were added as positive controls. To evaluate the functional avidity of T cells specific for the FH9 and FK10 peptides, the IFN-γ ELISpot assay was performed using 1 × 10^5 cells / well and serial dilutions (10^2 to 10^{-5} μg/ml) of each peptide were tested in duplicate. Spots were counted using an automated ELISpot plate reader (AID Systems, Germany) using ImmunoSpot software. Results were considered positive if they exceeded the mean of negative wells plus 3 standard deviations. Functional avidity was defined as the peptide concentration required to achieve 50% of the maximal response (EC_{50}) expressed in ng/ml and calculated using Graphpad Prism software version 8.

HLA class I tetramer staining

Biotinylated HLA-A*02:01 monomers refolded with FH9 and FK10 were obtained from the NIH Tetramer Core facility. Monomers were multimerized with streptavidin-PE or streptavidin-APC using previously described methods (Altman et al., 1996). Thawed PBMC were stained with tetramers at 37°C for 20 mins, followed by cell surface staining with CD3, CD8 and Aqua Live/Dead at room temperature for 15 mins. Samples were fixed in 2% paraformaldehyde and acquired on a CyAn flow cytometer. A minimum of 1000 events was acquired. In selected experiments, tetramer-positive cells were sorted using a MoFlo XDP cell sorter (Beckman Coulter).

QUANTIFICATION AND STATISTICAL ANALYSIS

Group medians were analyzed using Friedman's test. Curve-fitting was performed using the linear-quadratic model (Chadwick, 1973). Inter-subject variation was explored using linear regression analysis. All statistical analyses were performed using Graphpad Prism software, version 8.